

HIGH-SPEED WAVE-PIERCING CATAMARAN GLOBAL LOADS DETERMINED BY FEA AND SEA TRIALS

(DOI No: 10.3940/rina.ijme.2019.a2.522)

I Almallah, J Lavroff, D S Holloway and M R Davis University of Tasmania, Australia

SUMMARY

Wave-piercing catamaran hull forms are widely used for high-speed ferry applications due to the hull slenderness, suitable for achieving high speeds. The global loads acting on these craft are of great interest as there is limited knowledge on determining the magnitude of the loads, in particular when operating in random sea conditions. Longitudinal and transverse bending moments as well as pitch connecting moments and hull torsion loads act on the hull simultaneously. This paper investigates the estimation of these global loads from full-scale catamaran sea trials strain gauge data using finite element methods. Det Norske Veritas (DNV) load cases are applied to a finite element model in order to determine the conversion between local strain values observed during sea trials and prevailing global loads. Comparisons are thus made of global loads determined from strain data collected from sea trials with DNV global load cases. The results show that this method is relatively reliable for the prediction of hull global loads in the absence of slamming. Comparisons have been made for different heading angles. The quasi-static design loads are important during the ship design stage, as they are good proxies in wavelengths comparable to the hull length for rationally determined loads obtained from a first-principles dynamic analysis. The broad aims here are to demonstrate the use of strain sensor data obtained during sea trials for determination of global sea loads, to reconcile the loads thus determined with DNV load cases and thereby to improve the accuracy of the predicted loads used in design to increase the structural efficiency of vessel design.

NOMENCLATURE

L	Length of the craft (m)
β	Heading angle relative to waves ($^{\circ}$)
θ	Pitch angle ($^{\circ}$)
φ	Roll angle ($^{\circ}$)
M_{tot}	Longitudinal bending moment (LBM) (kN.m)
M_S	Transverse bending moment (TBM) (kN.m)
M_P	Pitch connecting moment (PCM) (kN.m)
M_t	Twin hull torsional moment (TM) (kN.m)
M_{SW}	Still water moment in loading condition (kN.m)
B_{WL2}	greatest moulded midship breadth of the hulls at the fully loaded waterline measured at $L/2$ (m)
B_m	Tunnel breadth between the hulls (m)
C_B	Block coefficient
C_W	Wave coefficient
Δ	Fully loaded displacement of the vessel (tonnes)
a_{cg}	Vertical design acceleration at LCG (m/s^2)
b	Transverse distance between the centrelines of the two hulls (m)
σ	Stress (Pa)
ε	Strain
E	Young's modulus (Pa)
F_x	Longitudinal compression force (N)
A	Sectional area at midship (m^2)
I	Second moment of area about y -axis (m^4)
z	Height measured from vertical neutral axis at midship (m)
H_w	Wave height (m)
v	Ship speed (knots)

1. INTRODUCTION

Ships encounter many types of global loading, including bending moment, shear and dynamic wave slamming loads, that are known to exert the peak nonlinear loads

acting on the vessel. Motion and wave induced loads are reported in many research papers and thesis reports due to the existing limitations in analysis for predicting the peak loads for vessel design purposes (Bashir et. al 2013 and Lavroff, 2009). During the design stage of the hull structure of a high-speed catamaran, dynamic wave-induced loads are the most significant of all types of loads and the most extreme of these loads are those due to wave slamming.

Essential global design loads for high-speed monohulls consist of longitudinal vertical bending moments, vertical shear forces, and torsional moments. Multihull ships, especially catamarans, encounter global loads different from those of monohulls. Catamaran vessels require determination of loads for the cross-deck structure connecting the two hulls. Thus, in addition to determination of longitudinal bending moments and shear forces, the cross-deck structure requires determination of pitch connecting moment (PCM) and transverse bending moment (TBM) (Holloway et al., 2003; Faltinsen, 2005; Shama 2010). The longitudinal twisting moment or torsional moment is also of interest and there is presently no direct way of determining these loads without numerical analysis validated with reference to experimentally measured results.

Estimating and determining the global loads at full-scale requires a monitoring system with a large number of strain sensors and accelerometers to capture motions and loads that the ship encounters in many different sea states. Study of available full-scale measurement data for high-speed catamarans is essential for prediction of these global loads. Full-scale measurements are thus an important source of information for validating design rules and guidelines, as well as for formulating rule approaches and formulae. In particular, data from full-scale measurements is employed

for the validation of design assumptions, design loads and for calculation tools (Kahl, 2014).

Finite element analysis (FEA) is beneficial in this type of study to estimate the global response of the ship structure. Conversion of measured strain data to external loading forces and moments is performed on the basis of finite element analysis results. Through finite element analysis, load cases for different encountered sea directions can be investigated, but they are restricted here to a quasi-static type analysis.

Bashir et al., (2013) have used the results from the experimental 1.5 m model tests on a Deep-V hull form catamaran to validate the numerical prediction of the wave-induced loads in regular wave conditions. Their focus was on the longitudinal, side (transverse) and the vertical shear forces, along with prying and yaw splitting moments in stern quartering and beam seas on the cross deck structure. The validation showed reasonable agreement between experimental and numerical data, providing useful results for vessel design. However these model tests did not include any slamming loads.

Strain gauges responses of surface effect ships (SES) have also been investigated (Pran et al., 2000; Wang et al., 2001, Johnson et al., 1999, 2000). Data has been collected from sea trials tests performed on a Norwegian naval vessel SES. The vessel is a high-speed air-cushion catamaran (SES), 47 m long and 13.5 m wide. The instrumentation included more than 50 fibre optic Bragg grating strain gauges, as well as conventional resistive strain gauges and accelerometers. The relatively large number of strain gauges was central to determining the global deformation modes of the hull and local stress concentrations. The instrumentation was employed during seakeeping tests in smooth and rough seas off the Norwegian coast. The measurements enabled detailed characterisation of the vessel dynamic response to wave loading and comparison with Finite Element Analysis modelling of the ship.

Nielsen and Jensen (2011) performed an analysis of full-scale motion measurements to investigate comparisons with "traditional" predictions calculated directly from spectral moments, and revealed better agreement with measured data by applying this novel approach. The motion measurements were acquired from a set of sensors used for response monitoring of the research vessel Shioji-Maru. The vessel is monohull of length 46 m, beam 10 m, and displacement 659 t. However, it was noted that in the analysis only a limited set of full-scale data runs was studied and further verification of the novel approach is required.

Kefal et al. (2015) and Kefal and Oterkus (2016) studied the inverse Finite Element Method (iFEM), which is a new method for real-time reconstruction of full-field structural displacements and stresses in plate and shell structures that are instrumented with strain sensors. Hydrodynamic analysis of a containership was performed for beam sea

waves in order to calculate vertical and horizontal wave bending moments, and torsional wave moments acting on the parallel mid-body of the containership. Several direct FEM analyses of the parallel mid-body were performed using the hydrodynamic wave bending and torsion moments. Furthermore, strains measured experimentally were simulated by strains obtained from high-fidelity finite element solutions. The effects of sensor locations and number of sensors were assessed with respect to the solution accuracy. Displacement and stress monitoring of the Panamax containership was performed based on the iFEM method. The optimum locations for strain gauges were determined for each FEM each case. These numerical results have proved the method for monitoring stresses and strains for the Panamax containership.

Results of calculation of global loads for a 112 m Incat wavepiercing catamaran design were presented by Davidson et al. (2006). Longitudinal bending and pitch connection moments were derived from linear and non-linear motion and loads software packages FASTSEA, SWAN and BESTSEA. The computed results were compared with rule based loads and empirically derived loads based on full-scale measurements undertaken on similar types of vessels.

Evaluation of finite element modelling as a tool to predict sea loads has been performed for 98m Incat high-speed wave piercing catamarans based on sea trials data (Amin et al., 2008, and Amin, 2009). A recent developed method was used to investigate sea loads during trials, and the results from the FE analysis were compared to trials data. It was found that a good comparison of strain time histories of trial and finite element analysis was difficult to achieve. However, the FEA RMS strains were in good agreement with trials root mean square (RMS) strains and approached a correlation coefficient of 95.5% for perfect head sea conditions and 80.2% for head seas with a slight loading asymmetry. Comparing the time histories of trial strains with those from FEA was found to give low correlation. This was caused by the asymmetric variation of sea direction about a nominal head-seas heading.

Jacobi et al. (2014) investigated slam events and loads from similar sets of data records to those in this analysis for different wave headings, vessel speeds and sea states for the 98m Incat vessel. This database of slam events allowed slam occurrence rates to be found and the influence of vessel speed, wave environment and heading to be determined for a range of conditions.

In the reviewed research work, it can be seen that full scale measurements have been conducted to analyse ship responses in terms of both motion or structural responses. Global loads have been investigated through full scale monitoring coupled with finite element modelling. However, the direct conversion from measured strain data to global loads for high-speed wave-piercing catamarans has not yet been investigated.



Figure 1. Image of HSV-2 Swift Incat catamaran hull 061 (98m) (colour online)

The analysis presented in the present paper investigates sea trials data for the Incat Swift HSV-2 catamaran (Figure 1). The main goal of this analysis is to estimate the global torsional loads acting on high-speed wave-piercing catamaran as determined from the sea trials data. This is performed using the finite element models as provided by the Incat design office, Revolution Design. In collaboration with Revolution Design and Incat, it was agreed to develop finite element load cases for the 98m catamaran HSV-2 to replicate the load conditions encountered during these sea trials undertaken by the Naval Surface Warfare Centre Carderock Division (NSWCCD) and US Navy. The developed FE model and the calculated strains predicted are compared to the load cases and results as presented by the NSWCCD (Sikora et al., 2004 and Grassman, 2007) for validation. The purpose of the work here is to combine the method of the quasi-static analysis using FEM based on the DNV rules for comparison to the measured data at full-scale as a predictive tool for identifying the torsional loads acting on the vessel in the absence of slamming. Broadly, the work aims to demonstrate that selectively located strain gauges can be used during full scale sea trials to identify various components of global sea loads and to reconcile the loads as determined by DNV load cases.

The chart shown in Figure 2 represents the work process conducted in this FEA study. Load cases from DNV rules are applied to the FE model to develop the load transfer matrix. From this global loads are estimated using the sea trials runs and the load transfer matrix.



Figure 2 Process of work based on the development of a FEA model using the loads predicted by DNV.

2. HSV-2 SEA TRIALS

Incat catamaran HSV-2 Swift was extensively tested through a large number of sea trials runs by the US Navy and NSWCCD to assess motion and structural responses of the vessel at wide range of wave heights, wave periods, wave headings and ship speeds (Brady, et al., 2004). HSV-2 Swift is a high-speed wave-piercing catamaran manufactured by

Incat Tasmania Pty Ltd, Hobart, Australia and designed by Revolution Design Pty Ltd. The catamaran was designed and built according to DNV classification society rules. HSV-2 Swift's maximum designed speed is 42.0 knots.

The sea trials were set to establish safe operation limits for the high-speed vessel swift (HSV-2) based on performance measurements obtained in calm water powering trials and in rough water seakeeping and structural loads trials. The effect of activating the ride control system (RCS) was also recorded during these runs.

The trials consisted of 22 octagons, each occurring at a specific sea state, wave height and period. Each octagon consisted of five runs at different heading angles (the three remaining sides of the octagon were assumed to be equivalent by symmetry). Figure 3 shows how the angle is measured from vessel centreline and Table 1 shows the relative heading angles used during the sea trials runs. The main particulars of HSV-2 are presented in Table 2.

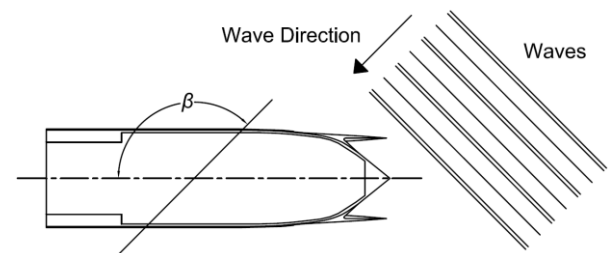


Figure 3 Heading angle of catamaran vessel relative to wave direction

Table 1 Relative wave-heading angle (Bachman, et al., 2004)

Sea wave headings	β°
Following Seas	0
Stern Quarter-Seas	45
Beam-Seas	90
Bow Quarter-Seas	135
Head-Seas	180

Table 2 Main particulars of HSV-2 Swift 98m catamaran

Main Dimension	Value
Incat hull number	061
Length overall	98 m
Waterline length	92 m
Overall beam	26.6 m
Beam of demihulls	4.48 m
Draft	3.44 m
Frame spacing	1.2 m
Fully loaded displacement	1697 t
Propulsion system ($\times 4$)	Water Jets
Power ($\times 4$ MDE)	7200 KW

2.1 INSTRUMENTATION OF HSV-2 SWIFT INCAT CATAMARAN

Seakeeping, structural and powering measurement instrumentation sensors were installed on HSV2 Swift with a data acquisition system (DAS) to support integrated measurements of structural response, ship motion, performance and manoeuvring capabilities. This is to develop the capacity to monitor structural response and ship motions to ensure safe operation during rough water sea conditions, including high-speed wave slamming.

Accelerometers were fitted to record ship motions in multiple directions including roll, pitch and yaw rates and vertical accelerations at the LCG of the vessel and bridge locations (Brady, et al., 2004). For the purpose of this study, pitch motion, roll motion and vertical acceleration (i.e. heave acceleration) were of greatest interest and yaw motion, transverse and longitudinal acceleration were not considered here. The identification of the pitch and roll angles of the vessel are determined from the schematic representation shown in figures 4 (a) and (b).

Wind and wave environment was also monitored and recorded. A Tsurumi Seiki Co., Ltd. (TSK) wave radar was installed on the centreline of the vessel at the bow of the ship to measure the height of the encountered waves.

HSV-2 was fitted with a large number of strain gauges to record different responses. These gauges have been divided into 4 groups. The first group was dedicated to primary global loads; each strain gauge in this group was numbered G1 – G16. The second group of strain gauges was dedicated to stress concentration at specific locations around the ship. The third group was dedicated to secondary loads such as wave impact in the forward region of the ship. The fourth group was dedicated to strain responses at specific locations such as the aft ramp, crane, and helicopter deck for example. The specific details of the first group of strain gauges, which was used in the present work, are described as follows:

Strain gauges G1-G16 were located at specific locations to pick up predominantly the corresponding response for longitudinal bending moment, pitch connecting moment and transverse bending moment. Figure 5 shows location of the strain gauges selected for analysis in this study, namely G2, G5, G11, G12 and G14. Their corresponding load responses are listed in Table 3. However, it would be appreciated that these gauges have only a dominant response to a particular global load and lesser responses to other global loads cannot be avoided.

Each strain gauge was positioned at the appropriate location to pick up a specific dominant loading response of the vessel. Strain gauge G5 was located at frame number 26, in the x - axis direction at approximately 31.2 m from the stern at the keel level to pick up primarily the longitudinal bending response of the ship, whether for sagging or hogging. Strain gauges G2 and G14 were

located at frame number 6, 7.2 m from stern, to measure dominantly the Pitch Connecting Moment (PCM) and Transverse Bending Moment (TBM) respectively. Strain gauge G2 was in the vertical z - axis direction and G14 was in the horizontal y - axis direction. Gauges G11 and G12 were fitted at the forward deck cut-out; both measure dominantly the Pitch Connecting Moment (PCM) and Transverse Bending Moment. Photographs of G2, G5 and G12 are shown in Figures 6–8.

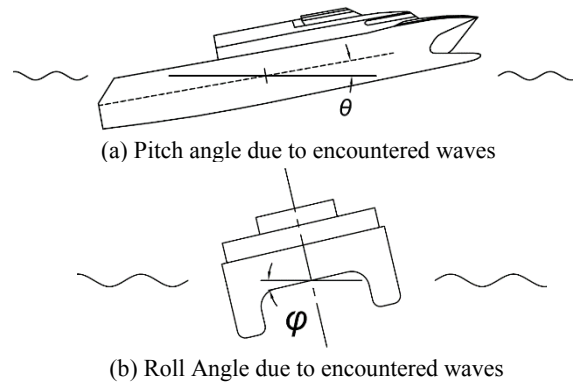


Figure 4 Catamaran motions response in pitch and roll

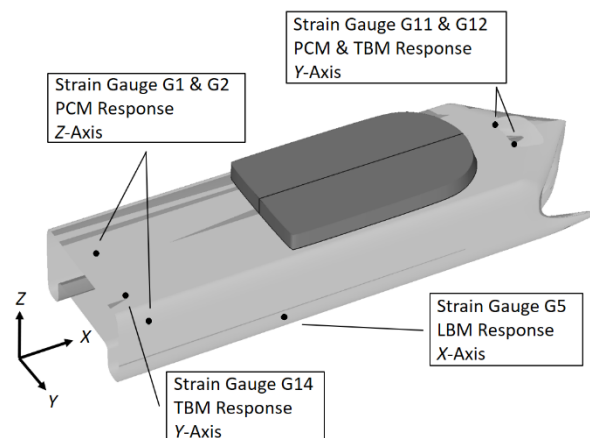


Figure 5 Strain gauges distribution

Table 3 Strain gauge intended load responses

Strain Gauge	Corresponding dominant load response
G2	Pitch Connecting Moment (PCM)
G5	Longitudinal bending load
G11 & G12	PCM and transverse bending loads
G14	Transverse bending load

2.2 PROGRAMME OF SEA TRIALS

Runs were selected for analysis in different headings, wave heights and speed, and consisted of head seas, bow quarter seas and beam seas, to study global loads change

over different sea conditions. Out of all the sea trials undertaken by the US Navy NSWCCD, Table 4 shows the selected run numbers with their corresponding octagon number, heading, wave height and speed that has been specifically selected for the purposes of this investigation. Each run was of duration 20 minutes.

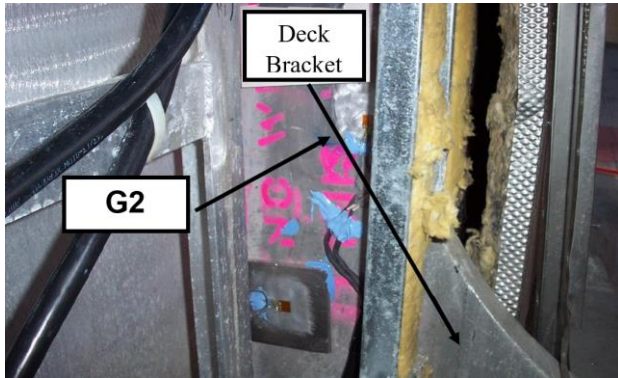


Figure 6 Strain Gauge G2 located at starboard deck bracket to measure Pitch Connecting Moment (PCM), Frame 6 (Kihl, 2006)

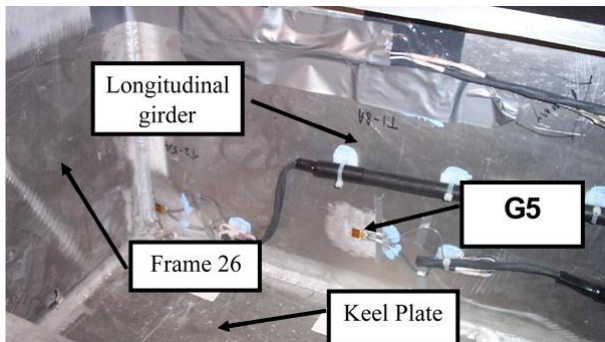


Figure 7 Strain Gauge G5 located at starboard keel Void 6 to measure Longitudinal Bending Moment (LBM), Frame 26 (Kihl, 2006)

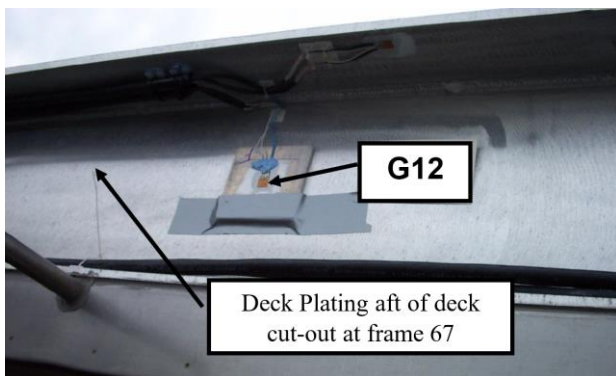


Figure 8 Strain Gauge G12 located at starboard foredeck cut-out Frame 67, to measure Pitch Connecting Moment (PCM) and Transverse Bending Moment (TBM) (Kihl, 2006)

With reference to Table 4, Run 70 was conducted in head seas, at ship speed of 20 knots, in Octagon number 3; the wave condition associated with this octagon was 2.5 m

significant wave height and 8.6 s wave period. A sample time record of 30 seconds has been selected from the run and the responses plotted in Figure 9. The 30 second window is selected to ensure that the motion response to wave loading has stabilized completely. Pitch and roll responses are measured at the LCG location and their angles have been recorded as presented.

Table 4 Specifications of selected sea trials runs on HSV-2 Swift 98 m Incat Catamaran

Run #	Octagon #	β (°)	H_w (m)	V (knots)
70	3	180	2.44	20
100	6	135	2.99	35
101	6	90	2.99	20

Normally at the forward 180° heading the pitch angle would have a significantly greater value than roll. In these results pitch ranges between $\pm 2^\circ$; roll angle is at a minimum, as roll motion is not usually associated with head seas. However, roll peaks of around 0.5° are observed, implying that there is some uncertainty regarding heading angle, or variability of the wave, which is inevitable in nominally head sea results. It is expected that there would be little roll motion associated with head seas but the roll motion observed is due to the randomness of the sea condition encountered at full-scale as would be expected. The sea heading is also estimated by observations made by the ship crew during the sea trial run itself and so it may not be exactly 180° as reported here. This issue has been addressed by Davis et. al. (2004) and Davis et. al (2005), and sea heading angles are estimated based on heave, pitch and roll motion responses of the catamaran. For each time record the instantaneous deck slope is estimated from pitch and roll values. Vertical heave velocity is multiplied by the deck slope magnitude at each point in the time record and a diagram of this product as a function of the deck slope direction was plotted. The data points on this diagram then indicated the sea direction as the angle for which the product was greatest in the negative sense.

As shown in Figure 9, strain records are plotted for gauges G5, G2 and G14 to show the vessel strain response at these different locations. The longitudinal bending response (gauge G5) is dominant over the other responses due to the increase in the hull girder loads in the longitudinal direction as a result of the head sea condition.

As shown in Table 4, run 100 was in bow quarter seas (135°), at speed of 35 knots. A sample set of time history data of this run is presented in Figure 10. It can be seen that responses of strain gauge G2 is higher than other gauges, which shows that this particular gauge is well capable of measuring the pitch connecting moment in the bow quarter seas test case. This is highlighted in the magnitude of the response with a peak of ± 100 microstrain, significantly greater than the other gauges.

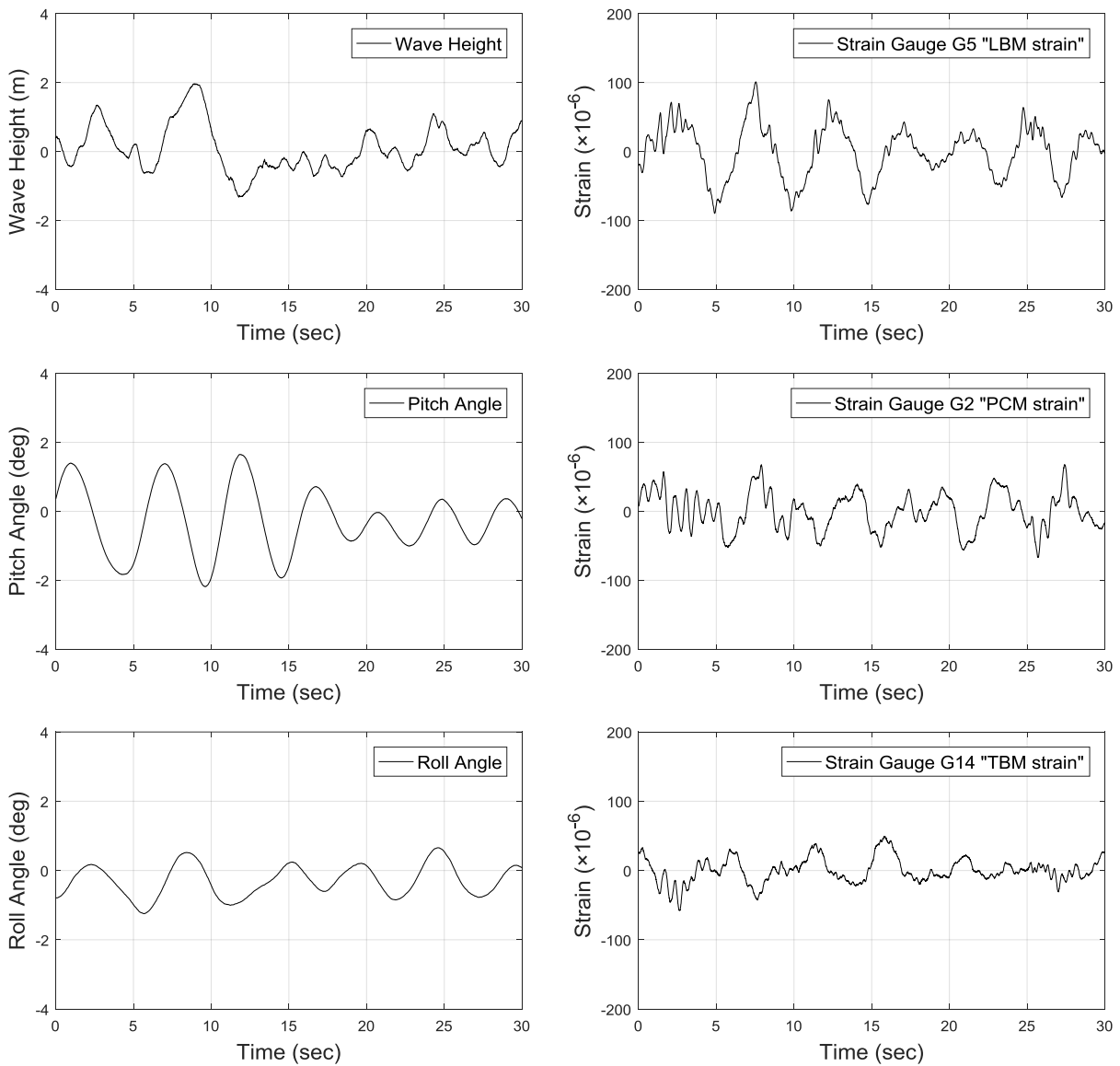


Figure 9. Run 70 Measured data (Octagon 3, Heading angle $\beta = 180^\circ$, Wave height $H_w = 2.44$ m, Speed $v = 20$ kn)

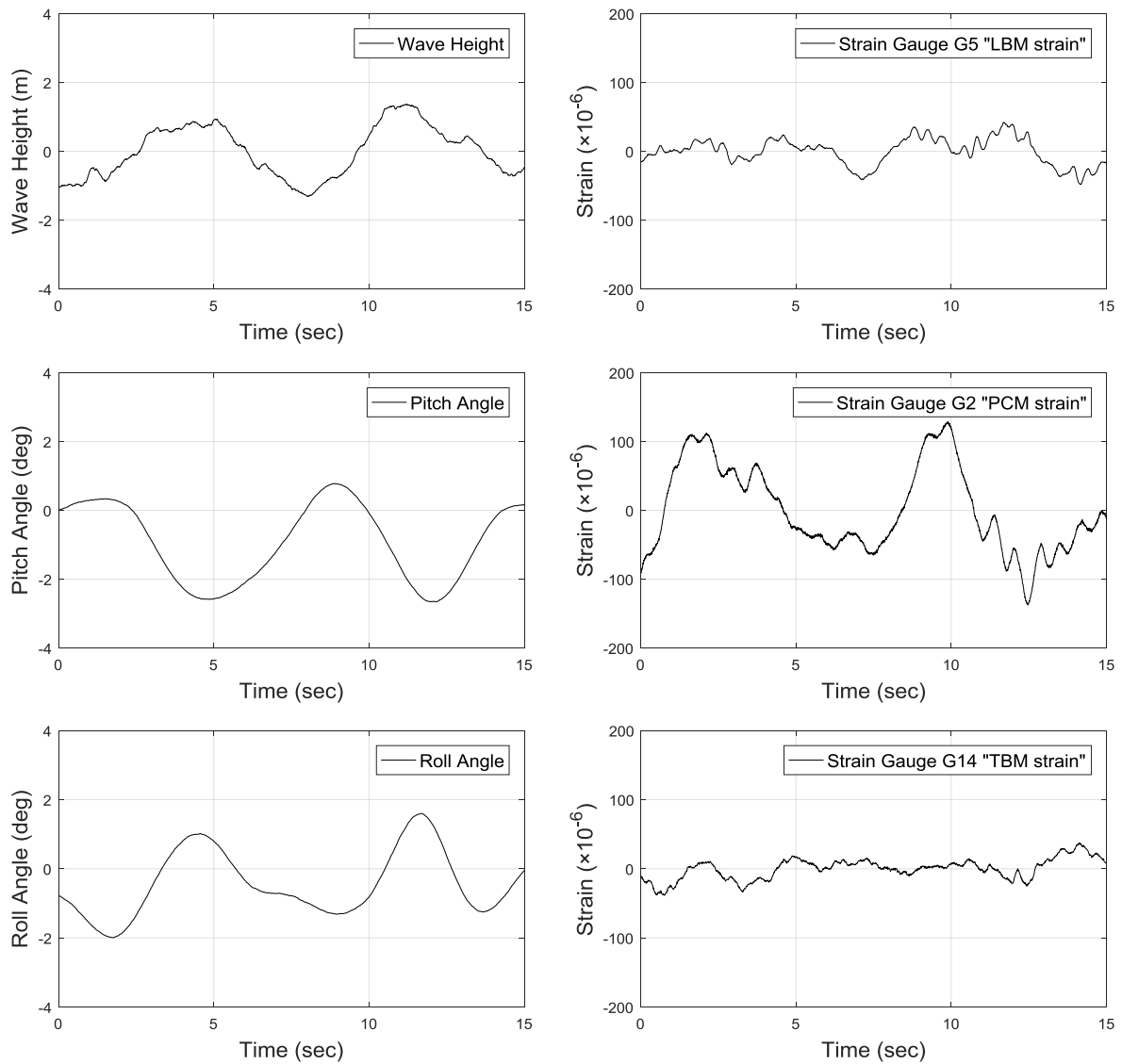


Figure 10. Run 100 Measured data (Octagon 6, Heading angle $\beta = 135^\circ$, Wave height $H_w = 2.99$ m, Speed $v = 35$ kn)

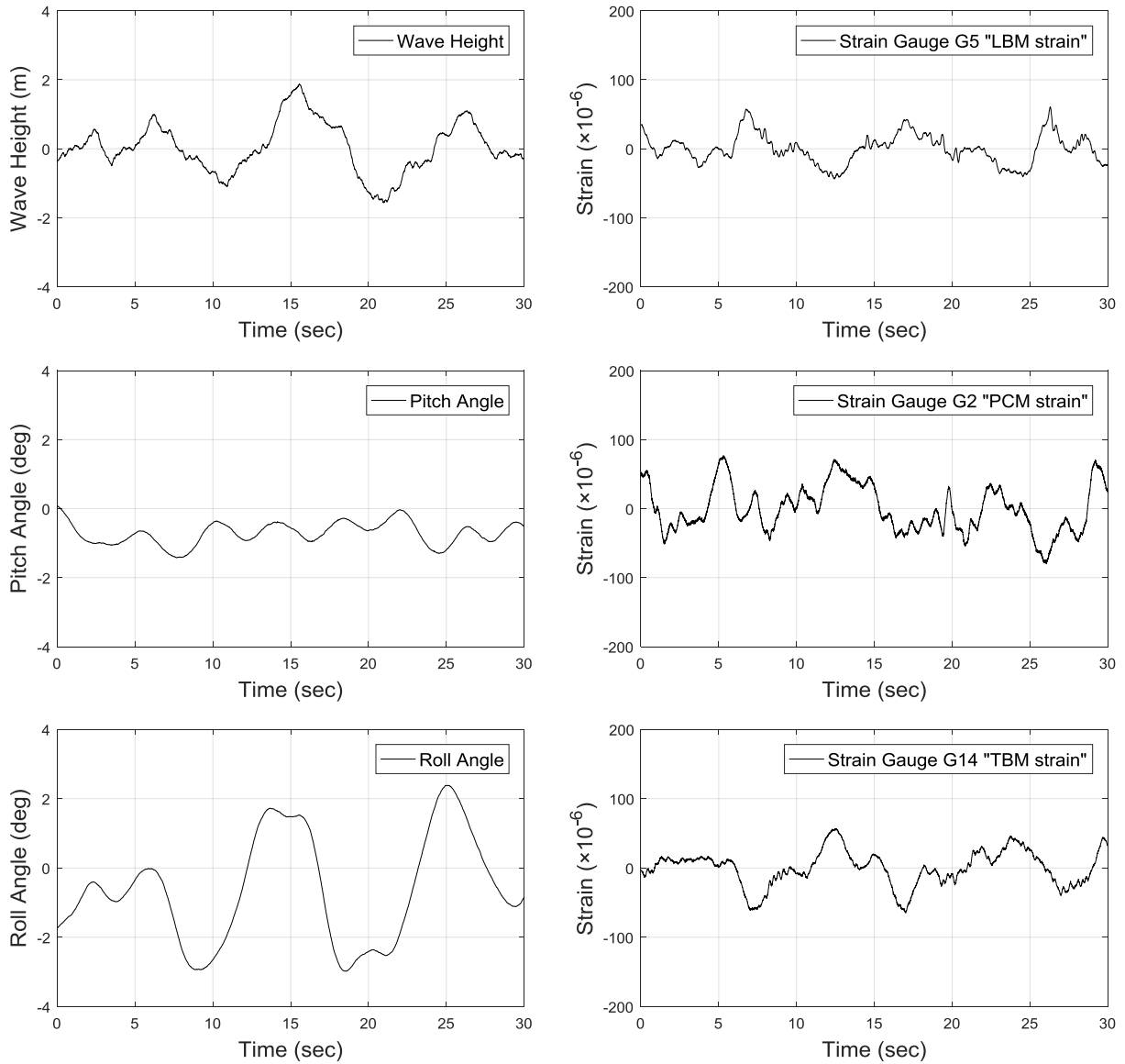


Figure 11. Run 101 Measured data (Octagon 6, Heading angle $\beta = 90^\circ$, Wave height $H_w = 2.99$ m, Speed $v = 20$ kn)

Run 101 was conducted in beam seas, at a speed of 20 knots. In this run, transverse bending is expected to be higher than the other runs, however, longitudinal bending is also of considerable magnitude. Figure 11 shows a time history sample of this run. Roll motion response is relatively larger than previous tested cases due to the beam-sea heading. Strain gauges responses remained at similar levels as in previous cases, except for G14, which has a larger response than runs 70 and 100, as would be expected for a gauge responding primarily to TBM in beam seas.

3. HSV-2 SWIFT FINITE ELEMENT ANALYSIS BASED ON DNV RULES

Several Finite Element Analysis (FEA) runs were performed to determine the static response of the HSV-2 Swift to design loads cases provided by the DNV rules formulae. The aim was to see how the design formulae relate to actual in-service loads.

The FE model of the Incat vessel was developed by the Revolution Design office, which is responsible for all designs associated with most of the Incat manufactured vessels. The FE model consists of around 2.0×10^5 nodes, and a total number of elements of 2.4×10^5 , which are of shell (quad and tri) and line type. Four load cases are presented here: (a) hogging longitudinal bending moment,

(b) sagging longitudinal bending moment, (c) transverse bending moment, (d) pitch connecting moment, and (e) still-water bending moment. The model is stabilized using inertia relief, to counter balance any non-equilibrium in the applied forces. In the output file, the inertia relief applied forces are checked for accuracy.

3.1 DNV LOAD CASES

The design loads for different modes of response to wave loading such as longitudinal bending, transverse bending and pitch connecting moment are provided by rule formulae. Figure 12 shows the load formulae and how these should be applied according to DNV rules.

Equations 1–5 (incorporated within Figure 12) show different rule formulae for hull girder design loads taken from DNV (2011).

The distribution of nodal forces in the FE model is aimed at replicating the same method of loads application as set by the DNV rules. For instance, the nodal forces in the longitudinal bending moment sagging case are distributed over $0.2L$ forward and aft of the catamaran as shown in Figure 12. For the transverse bending moment case and pitch connecting moment case, the nodal forces are applied to give the same moment direction as defined by the DNV rules.

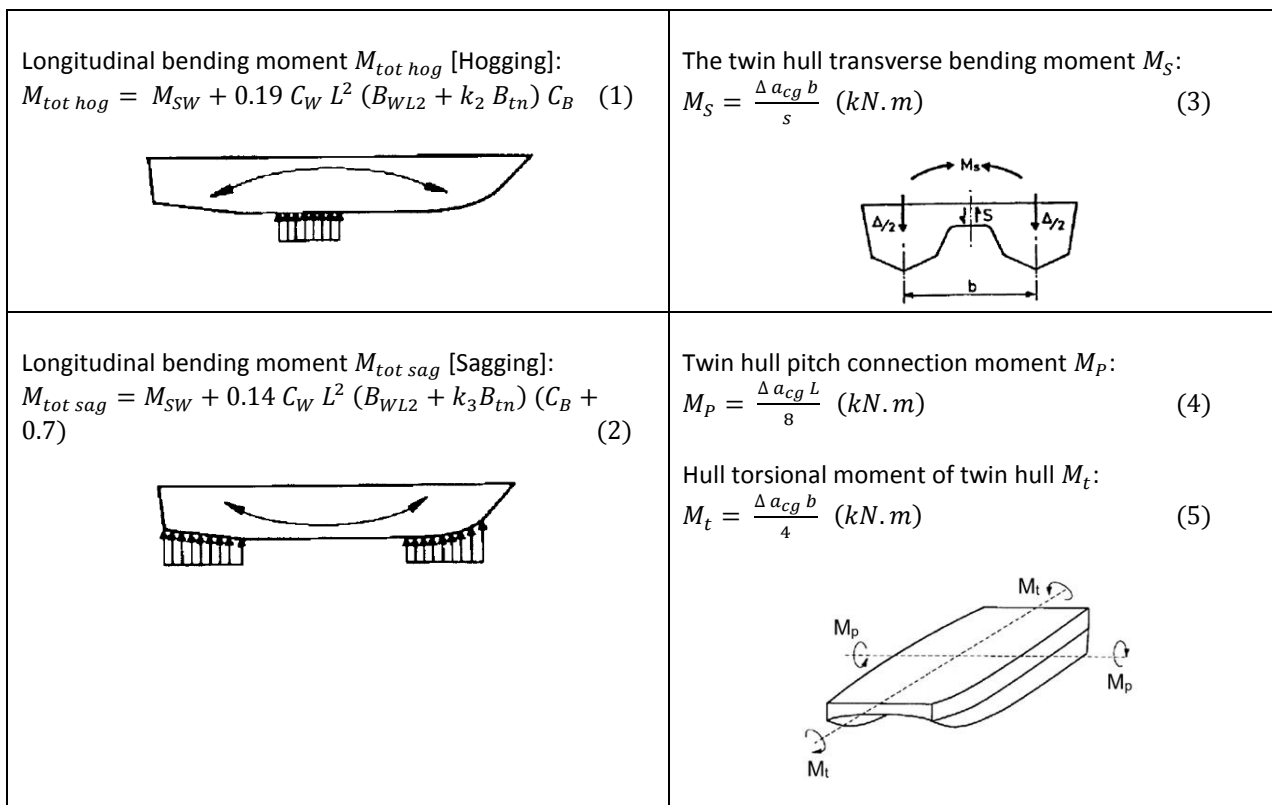


Figure 12. Loading formulae and diagrams as defined by (DNV 2011)

If M_{SW} is the still water moment in the most unfavourable loading condition, in kN.m, DNV rules estimate the most unfavourable condition that corresponds to a wave crest location. For the hogging case the wave crest is centred at the midship position, while for the sagging case the wave trough is centred at the midship position. C_W is the wave coefficient and L is the length of the vessel in meters (m), which is defined as the distance between perpendiculars. B_{WL2} is the net sum of the waterline breadths, in meters (m). k_2 and k_3 are empirical factors for the effect of cross structure immersion in hogging and sagging waves. B_{tn} is the breadth of cross structure (tunnel breadth) in meters (m). C_B is the block coefficient, Δ is the fully loaded displacement of the catamaran in tonnes, a_{cg} is the vertical design acceleration at the LCG (m/s^2), b is the transverse distance between the centrelines of the two hulls in meters (m) and s is the service restriction factor which depends on the class notation and service area and it ranges from 4 to 8.

The design loads have thus been estimated for HSV-2 Swift according to the formulae provided by the DNV rules. Table 5 shows the calculated load values.

Table 5 DNV hull girder loads as calculated for HSV-2 Swift 98 m Incat Catamaran

Load	Symbol	Value (MN.m)
Longitudinal Bending moment [Hogging]	$M_{tot\ hog}$	153.4
Longitudinal bending moment [Sagging]	$M_{tot\ sag}$	249.6
Transverse bending moment	M_S	68.8
Pitch connecting moment	M_P	191.7
Twin hull torsional moment	M_t	94.2

3.2 STRAIN LOAD CONVERSION

In order to convert measured strain signals into global loads, the principle of prismatic sections is applied and the section modulus approach is used to relate calculated strain to global moments or forces based on FEA. The commonly known relationship for load and calculated strain is shown in equation (6) (Hughes and Paik, 2010). Strain gauges are located so that each has a dominant sensitivity to a particular global load component. Measured strain are collected from FEA cases and have been related to the global load applied in the corresponding case.

The longitudinal bending moment M_y depends on the section properties at the midship section: second moment of area I and vertical height of deck or keel measured from neutral axis z and Young's modulus of elasticity E for Aluminum. Longitudinal strain ϵ_x also depends on the longitudinal compression force F_x ; F_x depends on the midship sectional area A and Young's modulus of elasticity E for Aluminum.

Figure 13 shows the cross-section of the catamaran with associated moments and forces and the corresponding longitudinal strain.

$$\epsilon_x = \frac{M_y \times z}{I \times E} + \frac{F_x}{E \times A} \quad (6)$$

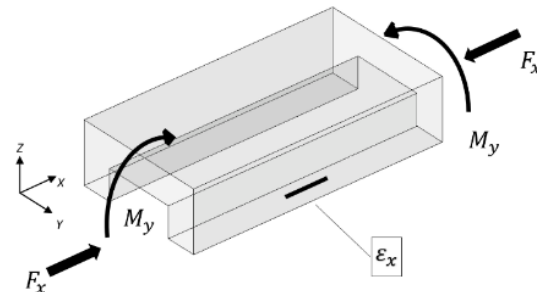


Figure 13 Schematic diagram showing bending and compression load on catamaran cross-section with corresponding strain identified in x-direction.

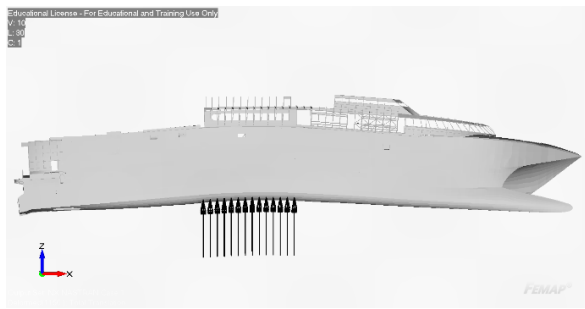
4. COMPARISON OF FINITE ELEMENT RESULTS FOR DIFFERENT LOADING CONDITION

Five linear-elastic static finite element cases have been undertaken to investigate vessel response to different loadings. Figure 14 shows the loading cases applied on the HSV-2 FE model and associated deflection mode. The FE results are compared with corresponding results of NSWCCD and the Revolution Design office. The response over different gauge positions is investigated to determine conversion methods from strain to global loads. For instance, the gauges placed at keel would respond most to longitudinal bending moment (LBM).

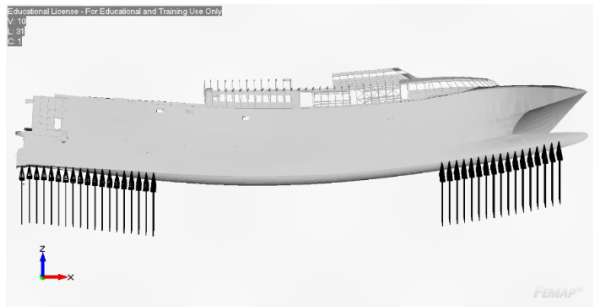
Strain values are collected from finite element results at the locations of the strain gauges to investigate the pattern of response at different modes of loading. A separate validation case has also been performed to investigate the effect of mesh refinement at the strain gauge location. The most suitable element size has been selected at strain gauges locations to ensure accurate strain results and less processing time.

Figure 15 shows the normalised strain responses from the various FE analyses. In the longitudinal bending moment sagging case, the dominating response is at strain gauge G5. This is to be expected as bending stresses reach a maximum at the midship area near the keel.

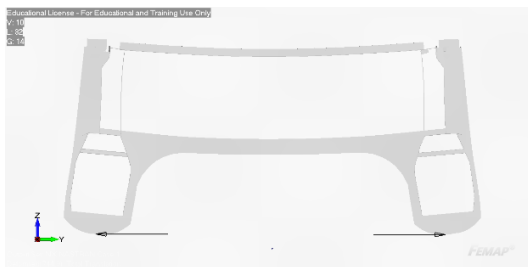
With the transverse bending moment case, the dominating response to this load is strain gauge G14. Although gauges G2, G11 and G12 are observed to have a high response for this particular case, they are not used to identify this type of load based on the strain gauge configuration mounted relative to the ship structure because they also pick up torsional loads.



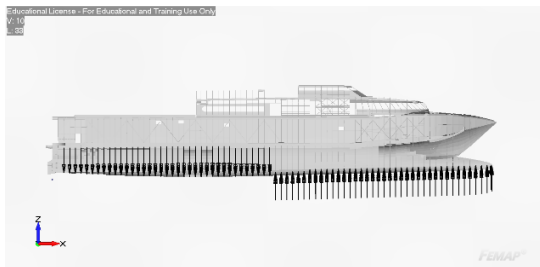
(a) Longitudinal bending moment hogging case



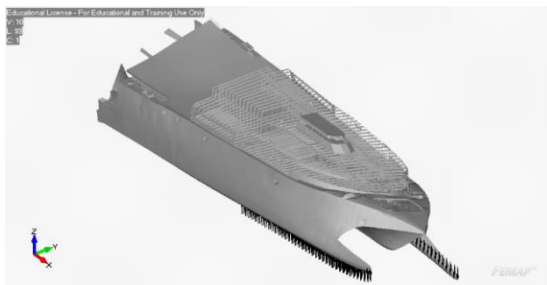
(b) Longitudinal bending moment sagging case



(c) Transverse bending moment case



(d) Pitch connecting moment case starboard loading



(e) Pitch connecting moment case deflection

Figure 14. Finite element analysis loading and deflection

The pitch connecting moment (PCM) case induces a high response in G2, G11 and G12. In this particular load case the G11 and G12 gauges have different signs of

measured strain signals. The difference between them (referred to as "Diff" on the far right-hand side of each chart) divided by two gives an estimate of the applied load. On the other hand this difference does not respond to any of the other load cases, which are all symmetric, therefore it provides a strong indicator of the PCM load case (there may be a very small response to these other load cases due to some slight structural asymmetry.) By reciprocity, the average value (referred to as "Avg" on the second column from the right-hand side of each chart) is zero in this particular case. The still water bending moment case is undertaken to analyse sea trials runs responses for various conditions. Gauge responses have been compared with those provided by Revolution Design and NSWCCD.

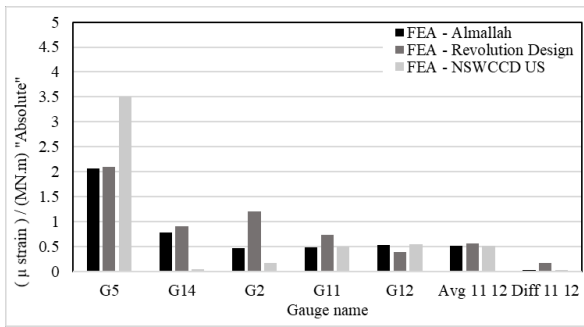
Some variations can be seen between these new Finite Element Analysis strain results and those provided by Revolution Design and NSWCCD. A key underlying reasons for this is that the finite element analysis results presented here use an FE model representing the actual HSV-2 ship and the rigidly attached superstructure of the sea trials as shown in Figure 16. However, the FE model used in the NSWCCD results models the HSV-X1 catamaran main hull with the superstructure removed, as shown in Figure 17. On HSV-X1 the superstructure was entirely resiliently mounted and thus didn't contribute to the main hull deformation stiffness.

The collection of strain responses at different gauge locations may result in certain fluctuations as strain values differ to a considerable value along elements near the strain gauge location. Consequently, the strain results presented are not expected to be exactly the same. Figure 18 shows stress results computed by the FEA at gauge G2, which correspond to Fr No. 6 bracket. It is noted that the mesh has been refined significantly in this region to resolve the variation. However, depending on the precise location of the gauge, the measured strain value can vary in the vicinity of the gauge position as indicated by the variation in stress as shown in the contour plot.

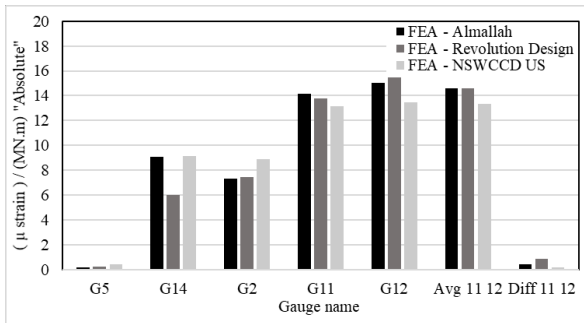
Another reason for the variation in results of the three independent finite element analyses presented is due to the application of loads that may not be exactly the same. For example, the nodal forces may not necessarily be distributed over exactly the same elements nor have the exact same value.

5. HSV-2 SWIFT INCAT CATAMARAN SEA TRIALS STRAIN RESPONSES

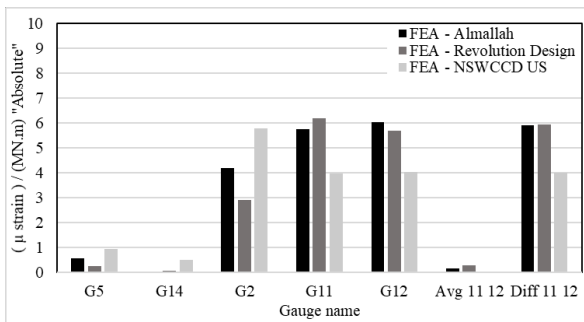
Several runs have been investigated from the sea trials undertaken on HSV-2 Swift in order to examine the trend of responses for comparison with those predicted from finite element analysis. During these trials each run at a particular heading relative the prevailing sea direction was of duration 20 minutes and the results for RMS values were determined using the full run records.



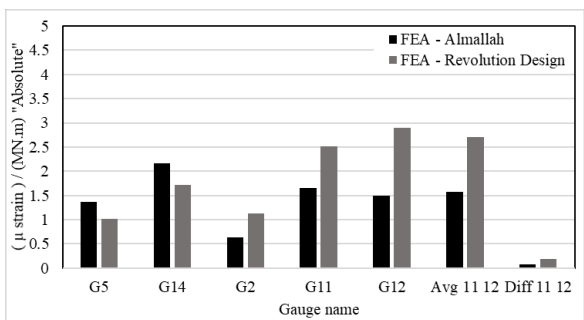
(a) Longitudinal bending moment Sagging case



(b) Transverse bending moment case



(c) Pitch connecting moment case



(d) Still water bending moment case

Figure 15 Comparison of Finite Element Analysis (FEA) results based on DNV Rules: Almallah (as calculated in the present investigation), Revolution Design and Naval Surface Warfare Centre Carderock Division (NSWCCD)

A sample of sea trials data during run 70 (Figure 9, in the absence of slamming) shows that the response of the strain gauges in head seas is mostly due to longitudinal bending. Figure 19 (a) summarises this run, and shows high values for strain gauge G5, while G2 and G14 have less magnitude. This measured data demonstrates correlation with the longitudinal bending moment sagging case predicted using FEA, shown in Figure 15(a).

Another sample of sea trials data was investigated based on measurements collected during run 100 (Figure 10, in the absence of slamming). Run 100 was conducted in bow quarter seas [$\beta=135^\circ$]. This heading angle corresponds to the maximum pitch connecting moment case, where strain gauge G2 has the highest response as shown in Figure 19 (b).

The beam sea case (Figure 11, run 101) was also investigated, and it can be seen in Figure 19 (c) that loading in the transverse direction is greater than the longitudinal direction, since strain gauges G2 and G14 have marginally higher values than strain gauge G5.

Results collected from this finite element analysis thus show generally good agreement of strain gauge responses for different loading directions and sea conditions presented in Figure 15.

Global loads are derived for different conditions for runs 70, 100 and 101. Conversion from strain values to global loads are performed using transformation matrix. The transformation matrix is obtained using strain responses from finite element analyses, as discussed in Section 3.2 and strain load relation derived from FEA as shown in Figure 15. Strain signals data from gauges G5, G14, G2, G11 and G12 are processed to find the corresponding global load.

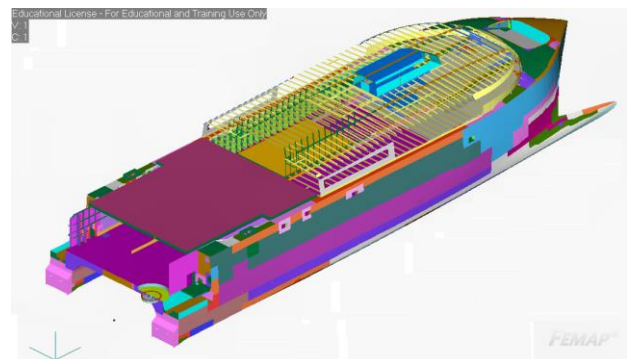


Figure 16 HSV-2 model used in Almallah FEA hull 061 98m (colour online)

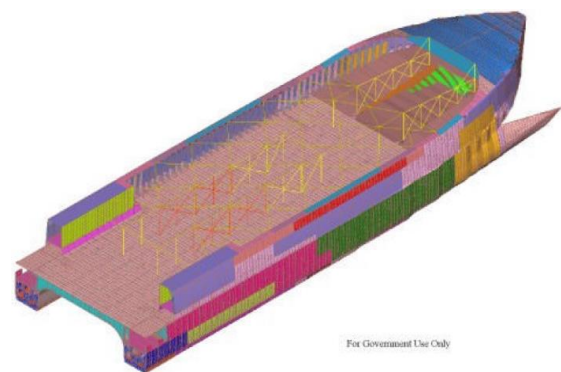


Figure 17 HSV-X1 model used in FEA by NSWCCD hull 050 96m (colour online) (Sikora et al., 2004)

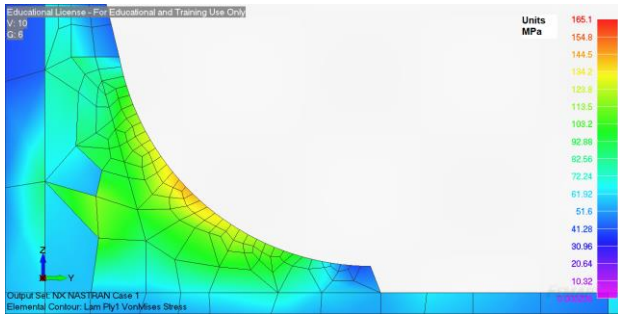
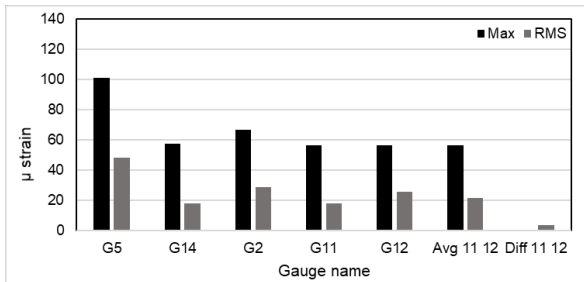
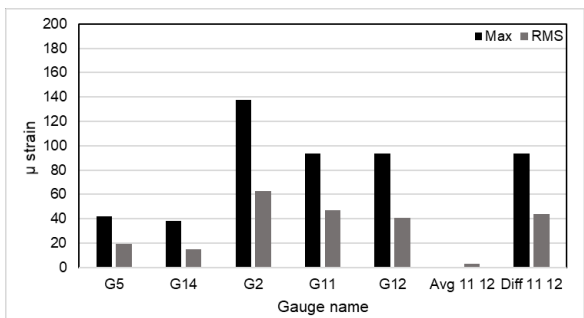


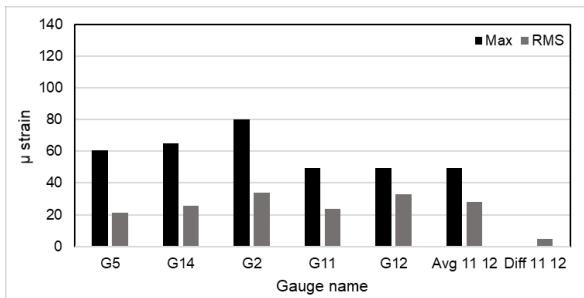
Figure 18 Finite element analysis (FEA) Von-Mises stress contours of deck bracket at frame (colour online)



(a) Head Seas (run 70)



(b) Bow Quarter Seas (run 100)



(c) Beam Seas (run 101)

Figure 19 Maximum and RMS values of strain during sea trials undertaken on HSV-2 Swift in the absence of slamming.

Figure 20 shows the derived longitudinal bending moment (LBM), transverse bending moment (TBM) and pitch connecting moment (PCM) for each of these sea trials runs. Run 70 was undertaken in head seas, so it is expected that the longitudinal bending moment (LBM) is the dominating global load acting on the catamaran hull. The value of transverse bending moment (TBM) in run 70 is however quite large as shown in Figure 20, since the hull is bending transversely simultaneously with longitudinal bending during the head sea case.

Run 100, undertaken in quarter seas (Figure 20) is expected to have a high value of pitch connecting moment since wave is approaching the boat diagonally from 135°. So PCM is the highest load value is this run of 60 MN.m as shown.

In run 101, which was conducted in beam seas, the predominant global load is the longitudinal bending moment (LBM), however this simply reflects that the vessel is long compared with its beam (in spite of being a catamaran). As waves are approaching the ship from the side, the transverse bending moment (TBM) is at its highest value compared with other headings. Also pitch connecting moment has a substantial value, as shown in Figure 20.

These measured sea trials results thus compare relatively well to the trends predicted by the Finite Element Analysis for each of the load cases considered using the DNV approach as discussed earlier.

Finally, the value of all of these global moments is compared with DNV rule load limit, and the percentage of each load to corresponding DNV load is plotted in Figure 21.

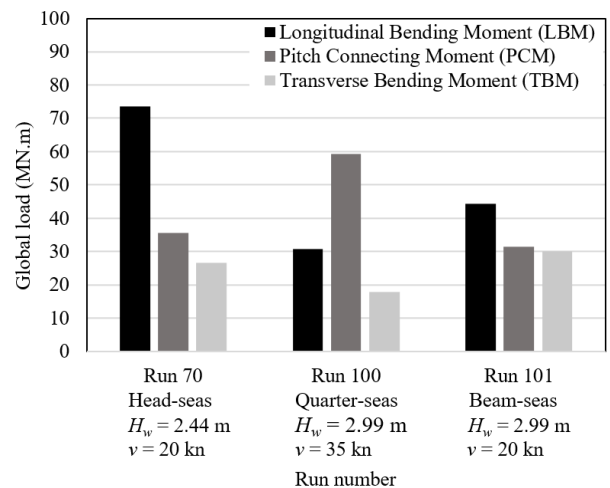


Figure 20 Global loads derived from sea trials runs on HSV-2 Swift 98 m Catamaran

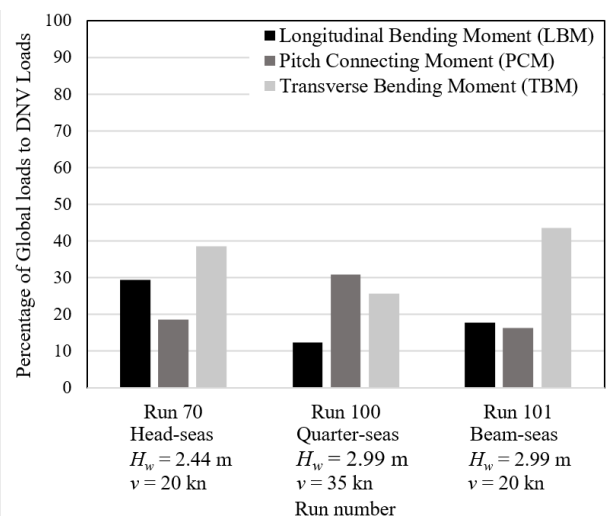


Figure 21 Percentage of Global loads to DNV Loads for different headings of sea trials runs

Through the three headings, the percentage of longitudinal bending moment (LBM) to DNV load is at highest value during the head-seas case. The percentage of pitch connecting moment to DNV rule is the largest at bow quarter-seas. It can be seen that the value of this percentage for transverse bending moment (TBM) is the highest for beam-seas and for head-seas as well. This means that the worst designated heading case for transverse bending moment (TBM) would be at these two headings.

The results also indicate that the loads measured during the sea trials as presented in Figure 21 quite clearly demonstrate significantly reduced values in the measured loads when compared to the predicted peak loads using the DNV loads case. Of course, these measured values are presented in the absence of slamming for the wave heights specified and it would be expected that the magnitude of the loads extracted from sea trials would increase in the presence of slamming.

6. CONCLUSIONS

Several finite element analyses have been undertaken to investigate global wave loads acting on a high-speed wave-piercing catamaran hull form. Loads within finite element analyses (FEA) are applied using DNV rules for twin hull loads.

Results showed a close trend compared with sea trials runs in different headings. Finite element analysis (FEA) using quasi-static loading is found to be sufficient for determining the trend of strain gauges responses observed in the sea trials runs. Furthermore, the conversion of strain data collected to corresponding global loads is achievable using finite element analysis.

The global loads are estimated for several sea trials runs undertaken at different heading angles. These prevailing global loads depend on the wave heading angle. Longitudinal bending moment (LBM) is the prevailing global load through encountered head and beam seas. Pitch connecting moment (PCM) is found to be greatest in bow quarter seas. The transverse bending moment (TBM) is found to have a substantial value in head seas although its highest value occurs in beam seas.

The global loads do not exceed 50% of DNV design load values since these are non-slamming loads. In slamming events these global loads increase dramatically.

The findings of this study were based on linear wave loading and quasi-static finite element analyses. However, to exactly simulate the sea trials responses, a much more sophisticated numerical method involving the complete vessel dynamics should be considered in future work. Computational fluid dynamics (CFD) coupled with structural loads response (McVicar et al., 2018) is a new approach that enables the simulation of non-linear wave slamming to predict the ship motions and global loads

before build whilst also identifying the peak loads. However, such coupled dynamic computations are more computationally time consuming compared to finite element analyses. The approach adopted here gives a time efficient approximation to the structural loads bearing in mind the difficulty in predicting exactly the sea conditions likely to be encountered.

7. ACKNOWLEDGEMENTS

The authors thank INCAT Tasmania Pty Ltd and Revolution Design Pty Ltd for their support towards this research work. Naval Surface Warfare Center, Carderock Division "NSWCCD" is also acknowledged for providing access to data collected from sea trials on HSV-2 Swift.

8. REFERENCES

1. AMIN, W., DAVIS, M., and THOMAS, G. A. (2008) *Evaluation of finite element analysis as a tool to predict sea loads with the aid of trials data*. Proceedings of High Speed Marine Vehicles, Naples, Italy, pp. 1-12.
2. AMIN, W., *Non-linear unsteady wave loads on large high-speed wave piercing catamarans*. PhD thesis, University of Tasmania, 2009.
3. BASHIR, M. B., TAO, L., ATLAR, M., and DOW, R. S. (2013). *Experimental and numerical investigation of the wave-induced loads on a deep-V catamaran in regular waves*. In ASME 2013 32nd International Conference on Ocean, Offshore and Arctic Engineering, American Society of Mechanical Engineers. DOI: 10.1115/OMAE2013-10212.
4. BACHMAN, R. J., WOOLAVER, D. A. and POWELL, M. D. (2004) *HSV-2 Swift Seakeeping Trials*, Naval Surface Warfare Center, Cardrock Division, US Navy, Report NO: NSWCCD-50-TR-2004/052, 2004.
5. BRADY, T. F., BACHMAN, R.J., DONNELLY M. J., and GRIGGS, D. B. (2004) *HSV-2 Swift Instrumentation and Technical Trials Plan*, Naval Surface Warfare Center, Cardrock Division, Report NO: NSWCCD-65-TR-2004/18.
6. DAVIDSON, G., ROBERTS, T., and THOMAS, G., (2006). *Global and slam loads for a large wavepiercing catamaran design*. Australian Journal of Mechanical Engineering 3(2), pages 155:164.
7. DAVIS, M. R., WATSON, N. L. and HOLLOWAY, D. S. (2004) *Measurement and prediction of wave loads on a high-speed catamaran fitted with active stern tabs*. Marine Structures,17(7):503-535,doi: <http://dx.doi.org/10.1016/j.marstruc.2005.01.003>.
8. DAVIS, M. R., WATSON, N. L., & HOLLOWAY, D. S. (2005). *Measurement of*

- response amplitude operators for an 86 m high-speed catamaran. *Journal of Ship Research*, 49(2), 121-143.
9. DET NORSKE VERITAS (DNV), (2011), Rules for High Speed, Light Craft and Naval Surface Craft.
 10. FALTINSEN O. M. (2005) *Hydrodynamics of high-speed marine vehicles*. Cambridge university press.
 11. HOLLOWAY, D. S., DAVIS, M. R., & THOMAS, G. A. (2003). *Rigid body dynamic hull bending moments, shear forces and PCM in fast catamarans*. In The 7th International Conference on Fast Sea Transportation (Vol. 2, pp. B57-B64).
 12. GRASSMAN J. M., (2007) *Evaluation of Incat HSV-2 Finite Element Model*, Naval Surface Warfare Center, Cardrock Division, Report NO: NSWCCD-65-TR-2004/22.
 13. HUGHES, O. F., & PAIK, J. K. (2010). *Ship structural analysis and design*.
 14. JACOBI, G., THOMAS, G., DAVIS, M. R. and DAVIDSON, G. (2014). *An insight into the slamming behaviour of large high-speed catamarans through full-scale measurements*. *Journal of Marine Science and Technology* 19(1), pages 15:32.
 15. JOHNSON, G. A., PRAN, K., WANG, G., HAVSGARD, G., and VOHRA S. T., (1999). *Structural monitoring of a composite hull air cushion catamaran with a multi-channel fibre Bragg grating sensor system*. In Proceeding of 2nd International Workshop on Structural Health Monitoring, Stanford, CA, pages 190:198.
 16. JOHNSON, G. A., PRAN, K., SAGVOLDEN, G., FARSUND, O., HAVSGARD, G., WANG, G., and JENSEN, A. E. (2000). *Surface effect ship vibro-impact monitoring with distributed arrays of fibre Bragg gratings*. In SPIE proceedings series, pages 1406:1411. Society of Photo-Optical Instrumentation Engineers.
 17. KAHL, A., (2014). *Full-scale measurements*. Technical report, DNV-GL.
 18. KEFAL A., and OTERKUS, K. (2016). *Displacement and stress monitoring of a panamax containership using inverse finite element method*. *Ocean Engineering* 119, pages 16:29.
 19. KEFAL A., HIZIR, O., and OTERKUS, E. (2015). *A smart system to determine sensor locations for structural health monitoring of ship structures*. In Proceedings of 9th International Workshop on Ship and Marine Hydrodynamics, Glasgow, UK.
 20. KIHLE, D. P. (2006) *JHSV Full-Scale Trials Based Spectral Fatigue Assessment*. NSWCCD-65-TR-2006/35, Naval Surface Warfare Center, Carderock Division, West Bethesda, MD.
 21. LAVROFF, J. (2009) *The slamming and whipping vibratory response of a hydroelastic segmented catamaran model*. PhD thesis, University of Tasmania.
 22. MCVICAR, J., LAVROFF, J., DAVIS, M. R., & THOMAS, G. (2018). *Fluid-structure interaction simulation of slam-induced bending in large high-speed wave-piercing catamarans*. *Journal of Fluids and Structures*, 82, 35-58.
 23. NIELSEN, U. D. and JENSEN, J. J. (2011). *A novel approach for navigational guidance of ships using onboard monitoring systems*. *Ocean Engineering* 38(2), pages 444:455.
 24. PRAN, K., JOHNSON, G., JENSEN, A. E., HEGSTAD, K. A., SAGVOLDEN, G., FARSUND, O., CHANG, C., MALSAWMA, L., and WANG, G. (2000). *Instrumentation of a high-speed surface effect ship for structural response characterization during sea trials*. In SPIE's 7th Annual International Symposium on Smart Structures and Materials, pages 372:379. International Society for Optics and Photonics.
 25. SHAMA, M. (2010) *Torsion and shear stresses in ships*. Springer Science & Business Media.
 26. SIKORA J. P., FORD, H. M., RODD, J. L. (2004) *Seaway Induced Loads and Structural Response of the HSV-2*, Naval Surface Warfare Center, Cardrock Division, Report NO: NSWCCD-65-TR-2004/11.
 27. WANG, G., PRAN, K., SAGVOLDEN, G., HAVSGARD, G., JENSEN, A. E., JOHNSON, G. A., and VOHRA S. T., (2001). *Ship hull structure monitoring using fibre optic sensors*. *Smart materials and structures* 10, pages 472-478. DOI: 10.1088/0964-1726/10/3/308.